Clinical Neurophysiology 129 (2018) 2191–2196

Contents lists available at ScienceDirect

Clinical Neurophysiology

journal homepage: www.elsevier.com/locate/clinph

Deep learning for detection of focal epileptiform discharges from scalp EEG recordings

Marleen C. Tjepkema-Cloostermans [a,*], Rafael C.V. de Carvalho [a,b,1], Michel J.A.M. van Putten [a,b,1]

[a] Department of Clinical Neurophysiology and Neurology, Medisch Spectrum Twente, Enschede, The Netherlands
[b] Department of Clinical Neurophysiology, University of Twente, Enschede, The Netherlands

See Editorial, pages 2186–2187

ARTICLE INFO

Article history:
Accepted 2 June 2018
Available online 9 July 2018

Keywords:
Deep learning
Convolutional neural networks
EEG
Epileptiform discharges
Epilepsy

HIGHLIGHTS

- Deep learning detects epileptiform discharges with sensitivities of 20–80% at 94–100% specificity.
- Deep learning has promise to detect epileptiform discharges with similar accuracy as human experts.
- Deep learning may cause a fundamental shift in clinical EEG analysis in the next decade.

ABSTRACT

Objective: Visual assessment of the EEG still outperforms current computer algorithms in detecting epileptiform discharges. Deep learning is a promising novel approach, being able to learn from large datasets. Here, we show pilot results of detecting epileptiform discharges using deep neural networks.
Methods: We selected 50 EEGs from focal epilepsy patients. All epileptiform discharges (n = 1815) were annotated by an experienced neurophysiologist and extracted as 2 s epochs. In addition, 50 normal EEGs were divided into 2 s epochs. All epochs were divided into a training (n = 41,381) and test (n = 8775) set. We implemented several combinations of convolutional and recurrent neural networks, providing the probability for the presence of epileptiform discharges. The network with the largest area under the ROC curve (AUC) in the test set was validated on seven independent EEGs with focal epileptiform discharges and twelve normal EEGs.
Results: The final network had an AUC of 0.94 for the test set. Validation allowed detection of epileptiform discharges with 47.4% sensitivity and 98.0% specificity (FPR: 0.6/min). For the normal EEGs in the validation set, the specificity was 99.9% (FPR: 0.03/min).
Conclusions: Deep neural networks can accurately detect epileptiform discharges from scalp EEG recordings.
Significance: Deep learning may result in a fundamental shift in clinical EEG analysis.

1. Introduction

Since the first recording of the human EEG by Hans Berger in 1924 (Berger, 1929), visual assessment by trained experts has remained the gold standard, despite the digital nature of EEG recordings. While visual analysis has proven to be invaluable (Schomer and Lopes da Silva, 2011), it has various limitations, including time-consuming review times, long learning curves, inter-observer variability and the need for specialized personnel (Lodder and van Putten, 2014; Faught, 1993). Visual analysis limits widespread use of long-term ambulatory recordings, although it has been established that this may improve diagnostic sensitivity for detecting interictal discharges (Askamp and van Putten, 2014; Geut et al., 2017). Furthermore, visual analysis is associated with significant error rates, ranging from 5% to 25% (Benbadis and Lin, 2008; Lodder and van Putten, 2014).

* Corresponding author.
E-mail address: m.tjepkema-cloostermans@mst.nl (M.C. Tjepkema-Cloostermans).
[1] All three authors contributed equally.

https://doi.org/10.1016/j.clinph.2018.06.024
1388-2457/

This has driven the need for computer-assisted EEG interpretation, and many researchers developed "hand-made" features to detect interictal discharges or other relevant features from scalp EEG recordings (Gotman et al., 1997; van Putten, 2007; van Putten et al., 2005; Le Van Quyen and Bragin, 2007; Halford, 2009; Lodder and van Putten, 2013; Scheuer et al., 2017; Wilson and Emerson, 2002). In addition, techniques have been proposed for real-time analysis of the EEG in patients monitored in the ICU (Cloostermans et al., 2011), or to assist in predicting recovery from postanoxic coma (Tjepkema-Cloostermans et al., 2013, 2017). Although successful in these domains, routine interpretation of human EEG in the clinic is by visual assessment, generally outperforming any method proposed thus far. Apparently, the features of the multivariate time series used in visual assessment by trained experts are very difficult if not impossible to design explicitly.

Unlike other approaches, deep learning does not need an explicit recipe for a particular feature. By providing sufficient data, it can learn a hierarchical feature representation automatically: it effectively learns by example. This makes it a very powerful candidate method to process the large amount of digital EEG data currently available. Recent advances in deep learning, have shown impressive results in e.g. image classification (Bengio et al., 2012; LeCun et al., 2015). Deep learning has also promising applications in biology and medicine. Examples include plant-phenotyping (Pound et al., 2017), analysis of ECG signals (Übeyli, 2010), assessment of ultrasound images of breast lesions (Cheng et al., 2016), classification of skin lesions (Esteva et al., 2017), or diagnosing breast cancer (Golden, 2017).

Because of the complexity of the techniques deep learning comprises, the number of parameters increases up to millions. Previous attempts with traditional artificial neural networks from the 1980s and 1990s were limited in complexity and resources, and although deep learning has been developed in the 1990s, a reliable way to train the networks was missing at that time. Due to more recent developments in dedicated algorithms for training and the use of graphical processing units, deep learning became more relevant the last 5–7 years. Two of the most widely used types of deep learning architectures are convolutional neural networks (CNNs) and recurrent neural networks (RNNs). CNNs are motivated by Hubel and Wiesel's work on the cat visual cortex (Hubel and Wiesel, 1963) and are constructed to process input data, e.g. images, as multidimensional arrays, preserving spatial information. CNNs typically contain several convolutional and pooling layers in between the input layer (receptive field) and the output layer. This architecture allows learning an increasing number abstract features at many scales, ranging from small edges, to object parts, and finally entire objects. Recurrent neural networks (RNNs) are comprised of memory cells. Training and assessment takes into account not only data currently being processed, but also data that came before, judging the old data according to when it was seen and how coherent it is with the other data. Currently, the most common form of a RNN is to use a Long Short-Term Memory (LSTM) architecture, introduced by Hochreiter and Schmidhuber in 1997 (Hochreiter and Schmidhuber, 1997). These networks excel at predicting and classifying time-series, used e.g. in speech recognition (Sak et al., 2014) and text processing (Graves, 2013).

In this pilot study, we explore whether deep learning allows detection of interictal discharges from scalp EEG recordings. Such an approach is fundamentally different from using explicit features, and mimics how EEG expertise is obtained in the clinic: the novice is trained by exposure to many examples, supervised by an expert.

2. Methods

2.1. EEG data and pre-processing

From our digital EEG database, we randomly selected 50 EEGs that were classified as normal and 50 EEGs that contained focal interictal epileptiform discharges (sharp waves, spikes, spike-slow-waves or polyspike-waves: IEDs). This was done by searching for the terms "normal EEG" and "focal epilepsy" in the conclusion of the clinical report. Subsequently the complete clinical report and the EEG recording itself were reviewed by the clinical neurophysiologist to confirm. All EEGs were obtained as part of routine care, and anonymized before further analysis. The used data was heterogeneous, including both routine 20 min recordings and long-term ambulatory registrations with periods of sleep. Patients aged 4–72 years.

The EEGs with focal epileptiform discharges were reviewed again by an experienced clinical neurophysiologist (MvP), who annotated all epileptiform discharges. The clinical neurophysiologist was able to review the complete EEG in different montages, typically the bipolar longitudinal, Laplacian and common average montages. Subsequently, all interictal discharges were extracted as 2 s epochs. The parts of the EEGs without epileptiform discharges were discarded. From all 50 EEGs classified as normal, the complete recording was divided into non-overlapping epochs of 2 s.

As a next step, the data was divided into a training set, comprised of 80% of the EEG recordings (41,381 epochs, including 1478 IEDs), and a test set (8775 epochs, including 337 IEDs). We did not mix samples from the same patients between data-sets: all epochs from the same patient were used either for training or testing. Data were filtered in the 0.5–35 Hz frequency range (to reduce EMG artifacts and 50 Hz noise) and re-referenced to both a longitudinal bipolar montage and a source Laplacian. Downsampling to 125 Hz was performed to reduce the input size and thereby the complexity of the network, resulting in 18×250 matrices for the longitudinal bipolar montage and 19×250 matrices for the source Laplacian. All pre-processing routines were implemented in Octave.

For additional validation we used another independent set consisting of 12 EEGs from patients without epilepsy (divided into 11,782 epochs of 2 s) and 7 EEGs from patients with epilepsy, where all IEDs were annotated. Subsequently, the EEG was divided into non-overlapping epochs of 2 s, resulting in 93,762 epochs of which 536 were labelled as IEDs.

2.2. Deep learning architectures

To preserve the spatiotemporal nature of the EEG recordings, we implemented deep neural networks using convolutions (1D and 2D) and/or LSTMs. We used 5 main archetypes: 1D CNNs, 2D CNNs, LSTMs, 1D CNNs with LSTMs and 2D CNNs with LSTMS. For each archetype several models were trained. Input to these models were the preprocessed 2 s epochs, thereby all channels of a particular EEG epoch were fed to the network at once. This allows the network to evaluate the combination of channels, instead of classifying each channel separately, similar to a clinician who takes the spatial distribution of a waveform into account. Separate networks were trained for both montages.

Each architecture contained one or more fully connected terminal layers to deconstruct the features extracted from the upper layers and provide the output. Dropout layers (20–50%) were used in between. A softmax activation function was used for the last layer, providing the probability p_1 for the presence of an epileptiform discharge as the final output.

In 1D CNNs the filters of the convolutional layers are one dimensional (vectors). These models thereby initially evaluate each channel separately in the upper (convolutional) layers, while the terminal (fully connected) layers that form the "decision part" of the network combine the information from the different channels. In 2D CNNs the filters in the convolutional layers are two dimensional (matrices), and thereby directly combine both temporal and spatial information.

We implemented the network in Python using Theano and Keras and a CUDA-enabled NVIDIA GPU (GTX-1080), running on CentOS 7. Theano is one of the top numerical platforms for developing deep learning models, developed by the University of Montreal (The Theano Development Team, 2016). It is a Python library for fast numerical computation that can be run on the CPU or GPU (Brownlee, 2016). Keras is a minimalist and easy to use Python library for deep learning that can run on top of Theano (Chollet, 2015). We realized stochastic optimization using Adam (Kingma and Lei Ba, 2015) with learning rate = 0.0003, $\beta_1 = 0.91$, $\beta_2 = 0.999$, and $\epsilon = 10^{-8}$. As the loss function, the categorical cross-entropy was used.

We used the performance on the test data set to choose which trained models to discard or further improve. Final performance of the best model was established on the independent validation set.

2.3. Performance evaluation

The model provides the probability p_1 for the presence of an epileptiform discharge in a 2 s epoch. By varying the threshold for this probability, Receiver Operating Characteristic (ROC) curves were obtained. ROC curves were made for all models using the test set. The area under the curve (AUC) was used as an overall indicator of performance.

Final classification performance of the best model was evaluated on the independent validation set. For this evaluation, epochs with a probability $p_1 > 0.5$ were classified as abnormal, i.e. to contain an IED, while epochs lower than this threshold were classified as normal. Subsequently, sensitivity, specificity were calculated for each individual EEG in the validation set. Sensitivity was defined by the number of true positive (TP) epochs divided by the total number of epochs with IEDs. Specificity was defined by the number of true negatives (TN) epochs divided by the total number of epochs without IEDs. In addition, we calculated the false positive rate (FPR) per minute, which we defined as the total number of false positives (FP) divided by the duration of the EEG.

3. Results

We trained 346 different neural networks. While training of each model took approximately 2 h, successive classification for a 20 min EEG recording was obtained within 2 s, resulting in 600 labeled epochs. From the various archetypes, the 2D CNNs and 2D CNN-LSTMs outperformed the other ones in the test set with an AUC of 0.94 for the final 2D CNN model. The 1D CNNs and 1D CNN-LSTMs had inferior results (AUCs of 0.68–0.74). The difference in performance of 2D vs 1D CNNs indicate that spatial distribution of waveforms is an important characteristic of IEDs. The LSTMs did not perform better than random. The final model was evaluated in the validation set. Fig. 1 shows the architecture and Fig. 2 the ROC curve. As the differences between the Laplacian and longitudinal bipolar montages are small, only the results for the bipolar montage are shown.

Final classification for the EEGs of the validation set is presented in Table 1. For the EEGs with IEDs, we find an average sensitivity of 47.4% (range: 18.8–78.4%) with specificity of 98.0% (range 93.8–99.8%), which is associated with a false positive rate (FPR) of 0.6/min. For the normal EEGs, false positive epochs were detected in 2 out of 12 cases, with an average specificity of 99.9% (range 98.3–100%). This corresponds to 1–2 erroneously classified epochs per hour. Examples of correctly and incorrectly classified epochs are shown in Figs. 3 and 4.

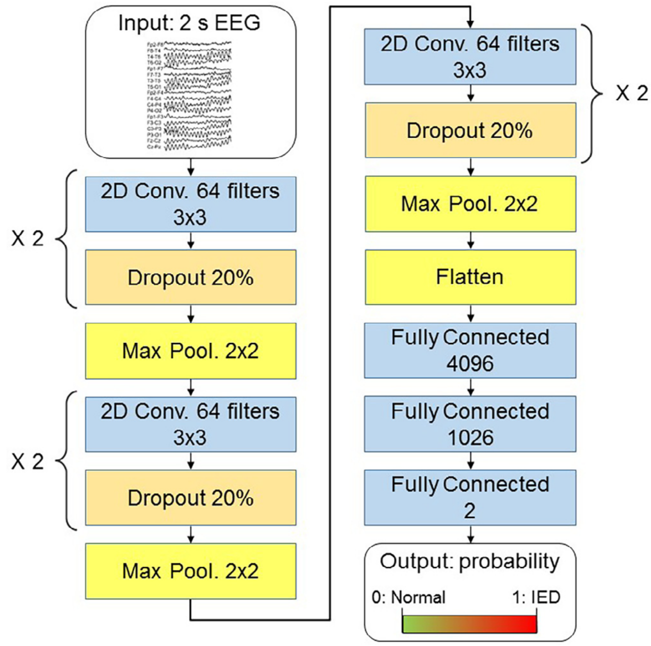

Fig. 1. Architecture of the final 2D convolutional neural network. The input processes EEG epochs with size 19 × 256. The output is the probability ([0–1]) that a particular 2 s epoch contains an epileptiform discharge. The total number of parameters is 9142859.

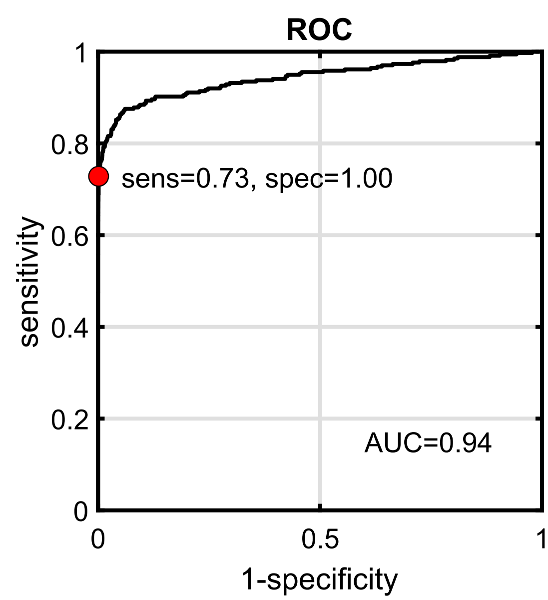

Fig. 2. Receiver operating characteristic (ROC) curve of the final 2D CNN model for the test set, with an area under the curve (AUC) of 0.94. The red marker indicates the performance of the network with a threshold of 0.5 for the probability of containing an epileptiform discharge. (For interpretation of the references to color in this figure legend, the reader is referred to the web version of this article.)

4. Discussion

Our pilot shows feasibility of convolutional and recurrent neural networks to detect focal epileptiform discharges in scalp EEG

Table 1
Overview of classification performance of the EEGs in the validation set after training with the EEGs in bipolar montage with a threshold of p = 0.5. IED = interictal epileptiform discharge; Sens = sensitivity; Spec = specificity.

Case	Epochs (n)	IEDs (n)	Sens (%)	Spec (%)
Epilepsy 1	768	162	78.4	95.2
Epilepsy 2	1193	2	50.0	98.8
Epilepsy 3	1228	32	18.8	98.7
Epilepsy 4	34,567	33	27.3	99.8
Epilepsy 5	22,271	130	20.8	98.9
Epilepsy 6	32,551	54	27.8	95.5
Epilepsy 7	1184	123	56.1	93.8
Normal 1	606	0	–	100
Normal 2	1596	0	–	100
Normal 3	602	0	–	100
Normal 4	660	0	–	98.3
Normal 5	602	0	–	100
Normal 6	1022	0	–	100
Normal 7	1133	0	–	100
Normal 8	949	0	–	100
Normal 9	1164	0	–	100
Normal 10	1519	0	–	100
Normal 11	610	0	–	100
Normal 12	1319	0	–	99.6

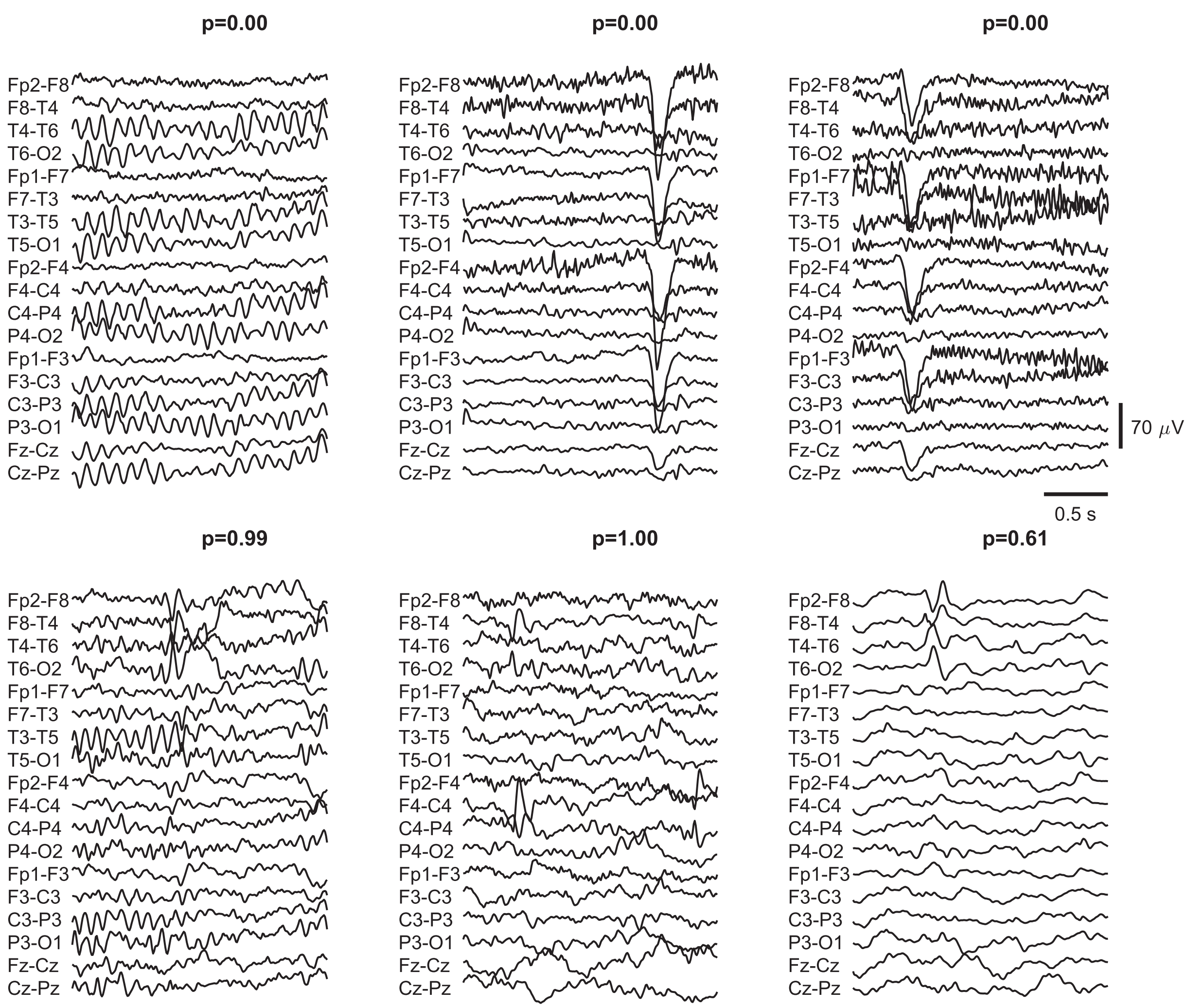

Fig. 3. Examples of correctly classified epochs from the validation set. The probability that the epoch contains an epileptiform discharge, is shown above each epoch. Top: Three correctly classified normal EEG epochs (true negative). Bottom: three epochs containing focal epileptiform discharges that were correctly classified (true positive).

recordings. In our evaluation set, we reached a sensitivity of 47.4% and specificities near 98–99% (FPR 0.03–0.6/min). Our results are up to par what is being reported in the literature using computer assisted detection of interictal discharges. For instance, using three existing computer algorithms, based on explicit feature extraction (Persyst 11, Persyst 12 and Persyst 13 and a large data set

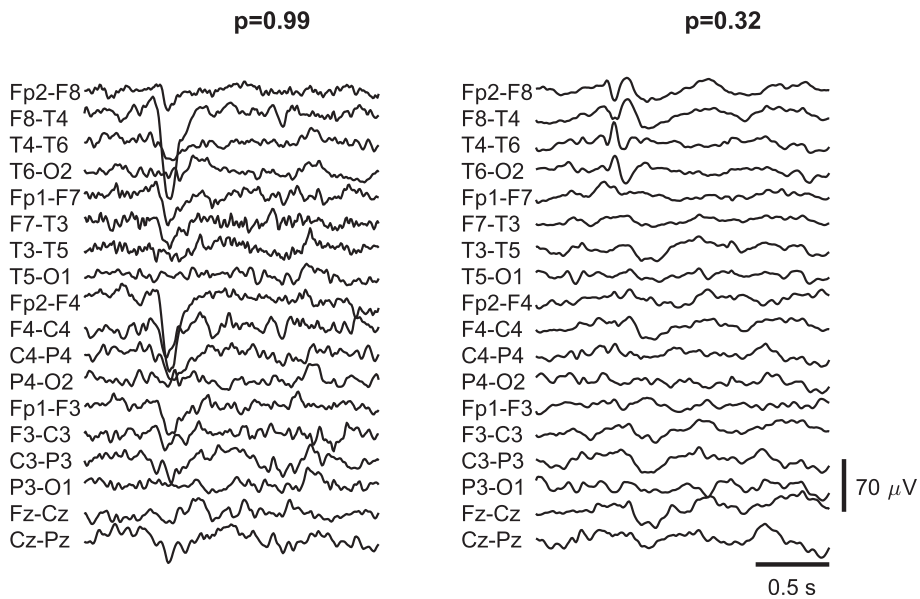

Fig. 4. Examples of two EEG epochs that were misclassified. The probability that the epoch contains an epileptiform discharge is shown above each epoch. Left: a normal EEG epoch classified as epileptiform discharge (false positive). Right: an epileptiform discharge that is not detected by the network (false negative).

containing 5474 spike events from 40 prolonged EEG recordings, Scheuer and co-workers reported sensitivities for these three algorithms of 17.6%, 19.2% and 43.9%, respectively (Scheuer et al., 2017). False positive rates of each algorithm corresponded to 0.53, 0.47 and 1.65 per minute. Although the data set used is different, our pilot results in slightly better sensitivities and false positive rates. Notably, the same study has 3 human reviewers that have only a fair level of agreement. They achieved sensitivities of 51.5%, 40.0% and 42.1% with false positive rates of 1.99, 0.97 and 0.8 per minute, respectively. This performance is also similar to our previous work using a database of smart templates Lodder et al. (2013) and that of others as summarized in a recent review (Halford, 2009).

Only a few studies explored spike detection with CNNs, all using data from a few patients, only. For instance, EEG from five patients was used using leave-on-out cross validation, resulting in an AUC of 0.95 (Johansen et al., 2016). Multi-class classification (including the class "sharp wave") with a semi-supervised deep belief net was explored using 11 EEGs from patients who underwent therapeutic hypothermia after cardiac arrest (Wulsin et al., 2011).

The larger number of false positives in EEGs of patients with focal epilepsy than in control EEGs suggests that the CNN detects features unnoticed by visual assessment (van Putten et al., 2018). Interictal EEG from patients with focal epilepsy, therefore, may contain other features than IEDs, that could assist in classification. In a computer model of dynamic networks, where the functional network was based on the extent of synchrony between EEG channels, such a biomarker for idiopathic generalized epilepsy was explored using resting state EEG, reporting a specificity of 100% at sensitivity 56.7% and 100% sensitivity at 65.8% specificity (Schmidt et al., 2016).

Displaying classifications during review would successively allow the electroencephalographer to judge the classification, including the possibility to reject or accept, as was previously proposed in Lodder and van Putten (2014). Thereby the user could adapt the used probability threshold. In this way, the epochs with the highest probability for containing epileptiform discharges could be shown first.

A unique feature of deep learning is the ability to learn from example, without explicit feature definitions, which is similar to how human experts review EEG recordings, and by training the network with more data, performance will typically become better (LeCun et al., 2015). In the current training and test set IEDs of 50 different patients were included. Since this number is probably too small to cover the complete variability in IED morphology, the model would benefit from a larger training set with IEDs from more epilepsy patients. Despite these potential limitations, we obtain good classification accuracies in the independent validation set, illustrating the high potential of deep neural networks. Although the variability of IEDs between patients may be larger than within patients, even within patients IEDs do vary in morphology. Further, the relation of the IED with the "background" is variable within patients, as well, and relevant for reliable detection. In future work, we will include more patients, as well, which will also allow us to study the relation between classification accuracy and the amount of IEDs used in the training from varying numbers of patients.

Since RNNs keep memory of previous processed data, they could benefit from longer EEG epochs, thereby having more context to compare the current processed data with (Schmidhuber, 2015). Therefore, detection of IEDs with RNNs, may be improved by processing the entire EEG, instead of using 2 s epochs, which is similar to a clinician who also prefer to review the complete EEG recording instead of a single 2 s EEG epoch. Increasing the training set and training the network with additional montages or combining the results from multiple models may also improve the classification accuracy. EEGs were down-sampled to 125 Hz, filtered in the 0.5–35 Hz range and divided in 2 s epochs. If changing these and other pre-processing parameters would result in better classification has not been explored, but it is not unlikely that the sensitivity for some artefacts may be reduced. Classification accuracy may also benefit from additional pre-processing, for instance by using techniques to reduce EMG contamination (Anderson and Doolittle, 2010).

It is sometimes argued that how decisions are taken by deep learning architectures is not explicit. Indeed, although the various "hidden layers" are essential to decode the input into components, the way this is performed and which particular features are encoded are generally not easy to elucidate. Recent advances, however, have made it possible to interact and experiment with them, allowing exploration of which particular components of features are relevant in classification (Wallach et al., 2015; Angermueller et al., 2016).

In sum, our pilot shows the feasibility of deep learning with a convolutional neural network to detect interictal epileptiform discharges from scalp EEG recordings. Further improvement in accuracy is possible if neural networks are trained with larger amounts of data and optimization of network architecture. Computer assisted EEG analysis with deep learning has also potential beyond identification of interictal discharges, e.g. in detecting slowing, asymmetries, and sleep stages (Tan et al., 2015). It is very likely that deep learning for EEG classification will more and more support the clinical neurophysiologist, with potential to even outperform human interpretation. This may ultimately induce a disruptive change in EEG interpretation, almost 100 years after Hans Berger recorded the first human EEG through the intact scalp in 1924 (Berger, 1929).

Conflicts of interest

M.J.A.M. van Putten is co-founder of Clinical Science Systems, a supplier of EEG systems for Medisch Spectrum Twente. Clinical Science Systems offered no funding and was not involved in the design, execution, analysis, interpretation or publication of the study. The remaining authors have disclosed that they do not have any conflicts of interest.

Acknowledgements

This work was financially supported by the Dutch Epilepsy Fund (Epilepsiefonds, grant number 16-08).

References

Anderson NR, Doolittle LM. Automated analysis of EEG: opportunities and pitfalls. J Clin Neurophysiol 2010;27(6):453–7.
Angermueller C, Pärnamaa T, Parts L, Stegle O. Deep learning for computational biology. Mol Syst Biol 2016;12(7):878.
Askamp J, van Putten MJAM. Mobile EEG in epilepsy. Int J Psychophysiol 2014;91(1):30–5.
Benbadis SR, Lin K. Errors in EEG interpretation and misdiagnosis of epilepsy. Eur Neurol 2008;59(5):267–71.
Bengio Y, Courville A, Vincent P. Representation learning: a review and new perspectives. IEEE Trans Pattern Anal Mach Intell 2012;35(8):1–34.
Berger H. Über das Elektrenkephalogramm des Menschen. Arch Psychiatr Nerven 1929;87(1):527–70.
Brownlee J. Deep learning with Python. Develop deep learning models on Theano and TensorFlow using Keras 2016;vol. 1.3. Machine Learning Mastery; 2016.
Cheng J-Z, Ni D, Chou Y-H, Qin J, Tiu C-M, Chang Y-C, et al. Computer-aided diagnosis with deep learning architecture: applications to breast lesions in US images and pulmonary nodules in CT scans. Sci Rep 2016;6(1):24454.
Chollet F. Keras; 2015. <https://keras.io>.
Cloostermans MC, De Vos CC, Van Putten MJAM. A novel approach for computer assisted EEG monitoring in the adult ICU. Clin Neurophysiol 2011;122(10):2100–9.
Esteva A, Kuprel B, Novoa RA, Ko J, Swetter SM, Blau HM, et al. Dermatologist-level classification of skin cancer with deep neural networks. Nature 2017;542(7639):115–8.
Faught E. Current role of electroencephalography in cerebral ischemia. Stroke 1993;24(4):609–13.
Geut I, Weenink S, Knottnerus ILH, van Putten MJAM. Detecting interictal discharges in first seizure patients: ambulatory EEG or EEG after sleep deprivation? Seizure 2017;51:52–4.
Golden JA. Deep learning algorithms for detection of lymph node metastases from breast cancer. JAMA 2017;318(22):2184.
Gotman J, Flanagan D, Rosenblatt B, Bye A, Mizrahi EM. Evaluation of an automatic seizure detection method for the newborn EEG. Electroencephalogr Clin Neurophysiol 1997;103(3):363–9.
Graves A. Generating sequences with recurrent neural networks. In: Proceedings of the 23rd ACM international conference on conference on information and knowledge management – CIKM '14. p. 101–10.
Halford JJ. Computerized epileptiform transient detection in the scalp electroencephalogram: obstacles to progress and the example of computerized ECG interpretation. Clin Neurophysiol 2009;120(11):1909–15.
Hochreiter S, Schmidhuber J. Long short-term memory. Neural Comput 1997;9(8):1735–80.
Hubel DH, Wiesel TN. Shape and arrangement of columns in cat's striate cortex. J Physiol 1963;165(3):559–68.
Johansen AR, Jin J, Maszczyk T, Dauwels J, Cash SS, Westover MB. Epileptiform spike detection via convolutional neural networks. In: 2016 IEEE international conference on acoustics, speech and signal processing (ICASSP). p. 754–8.
Kingma DP, Lei Ba J. Adam: a method for stochastic optimization. In: Proceedings of the 3rd international conference on learning representations (ICLR).
Le Van Quyen M, Bragin A. Analysis of dynamic brain oscillations: methodological advances. Trends Neurosci 2007;30(7):365–73.
LeCun Y, Bengio Y, Hinton G. Deep learning. Nature 2015;521(7553):436–44.
Lodder SS, Askamp J, van Putten MJAM. Inter-ictal spike detection using a database of smart templates. Clin Neurophysiol 2013;124(12):2328–35.
Lodder SS, van Putten MJAM. Quantification of the adult EEG background pattern. Clin Neurophysiol 2013;124(2):228–37.
Lodder SS, van Putten MJAM. A self-adapting system for the automated detection of inter-ictal epileptiform discharges. PLoS ONE 2014;9(1):e85180.
Pound MP, Atkinson JA, Townsend AJ, Wilson MH, Griffiths M, Jackson AS, et al. Deep machine learning provides state-of-the-art performance in image-based plant phenotyping. GigaScience 2017;6(10):1–10.
Sak H, Senior A, Beaufays F. Long short-term memory based recurrent neural network architectures for large vocabulary speech recognition. Interspeech 2014:338–42.
Scheuer ML, Bagic A, Wilson SB. Spike detection: inter-reader agreement and a statistical Turing test on a large data set. Clin Neurophysiol 2017;128(1):243–50.
Schmidhuber J. Deep learning in neural networks: an overview. Neural Netw 2015;61:85–117. <http://linkinghub.elsevier.com/retrieve/pii/S0893608014002135>.
Schmidt H, Woldman W, Goodfellow M, Chowdhury FA, Koutroumanidis M, Jewell S, et al. A computational biomarker of idiopathic generalized epilepsy from resting state EEG. Epilepsia 2016;57(10):e200–4.
Schomer DL, Lopes da Silva FH. Niedermeyer's electroencephalography: basic principles, clinical applications, and related fields, 6th Edition. 6th ed. Philadelphia: Lippincott Williams & Wilkins; 2011.
Tan D, Zhao R, Sun J, Qin W. Sleep spindle detection using deep learning: a validation study based on crowdsourcing. In: 37th Annual international conference of the IEEE engineering in medicine and biology society (EMBC). p. 2828–31.
The Theano Development Team. Theano: a Python framework for fast computation of mathematical expressions; 2016. Available from: arXiv:1605.02688>.
Tjepkema-Cloostermans MC, Hofmeijer J, Beishuizen A, Hom HW, Blans MJ, Bosch FH, et al. Cerebral recovery index: reliable help for prediction of neurologic outcome after cardiac arrest. Crit Care Med 2017;45(8):e789–97.
Tjepkema-Cloostermans MC, van Meulen FB, Meinsma G, van Putten MJAM. A Cerebral Recovery Index (CRI) for early prognosis in patients after cardiac arrest. Crit Care 2013;17(5):R252.
Übeyli ED. Recurrent neural networks employing Lyapunov exponents for analysis of ECG signals. Expert Syst Appl 2010;37(2):1192–9.
van Putten MJAM. The revised brain symmetry index. Clin Neurophysiol 2007;118(11):2362–7.
van Putten MJAM, Kind T, Visser F, Lagerburg V. Detecting temporal lobe seizures from scalp EEG recordings: a comparison of various features. Clin Neurophysiol 2005;116(10):2480–9.
van Putten MJAM, Olbrich S, Arns M. Predicting sex from brain rhythms with deep learning. Sci Rep 2018;8(1):3069.
Wallach I, Dzamba M, Heifets A. AtomNet: a deep convolutional neural network for bioactivity prediction in structure-based drug discovery; 2015. p. 1–11. Available from: arXiv:1510.02855.
Wilson SB, Emerson R. Spike detection: a review and comparison of algorithms. Clin Neurophysiol 2002;113:1873–81.
Wulsin DF, Gupta JR, Mani R, Blanco JA, Litt B. Modeling electroencephalography waveforms with semi-supervised deep belief nets: fast classification and anomaly measurement. J Neural Eng 2011;8(3):036015.